Article

Influence of Isothermal Annealing in the 600 to 750 °C Range on the Degradation of SAF 2205 Duplex Stainless Steel

Jaka Burja [1,2,]*[], Borut Žužek [1] and Barbara Šetina Batič [1][]

1   Institute of Metals and Technology, 1000 Ljubljana, Slovenia; barbara.setina@imt.si (B.Š.B.)
2   Department for Materials and Metallurgy, Faculty of Natural Sciences and Engineering, University of Ljubljana, 1000 Ljubljana, Slovenia
*   Correspondence: jaka.burja@imt.si; Tel.: +386-1-4701-981

Abstract: We studied the effect of isothermal annealing (600–750 °C, 1 to 1000 min) on the microstructure and mechanical properties of SAF 2205 duplex stainless steel. Impact toughness was found to be significantly more affected than hardness by annealing. Annealing at 750 °C for 1000 min resulted in a more than 90% decrease in impact toughness, while hardness only increased by 25%. Tensile strength increased up to 100 MPa, but elongation decreased by more than 50% under the same conditions. Sigma phase formation was minimal at lower temperatures (650 °C and below) but increased significantly at higher temperatures. At 750 °C and 1000 min of annealing, the ferrite content dropped from 50% to 16%. These findings suggest that annealing temperature and time need to be carefully controlled to avoid a reduction in impact toughness and ductility caused by sigma phase precipitation. The harmful effect of sigma phase precipitation on mechanical properties was directly shown.

Keywords: duplex stainless steel; sigma phase; precipitation kinetics; mechanical properties; isothermal annealing

1. Introduction

Stainless steels are valued for their corrosion resistance, which is mainly provided by the high chromium content (above 10.5% Cr) [1]. There are, however, depending on the classification, four to five groups: austenitic stainless steels, ferritic stainless steels, martensitic stainless steels, duplex stainless steels, and precipitation-hardened stainless steels (usually with an austenitic or a martensitic matrix). Austenitic stainless steels are generally the most corrosion-resistant and are the most widely used, with AISI 304 and AISI 316 being prime examples [2]. Ferritic stainless steels are less corrosion-resistant, but cheaper due to lower Ni contents, and easier to cold-work [3]. Martensitic stainless steels are the least corrosion-resistant but have the highest strength and hardness among stainless steels. Duplex stainless steels (DSSs) are less expensive and stronger than austenitic stainless steels while retaining high corrosion resistance due to their high alloying-element content [4,5]. Duplex stainless steels are valued for their excellent properties, including their high pitting and stress corrosion cracking resistance, resistance to intergranular corrosion, good mechanical strength, corrosion fatigue resistance, wear resistance, superplastic behavior, and acceptable weldability [6–8].

However, most of the issues concerning duplex stainless steels arise from the fact that they are highly alloyed, with >20% Cr, >0.1% N, and >1% Mo. Duplex stainless steel processing presents specific challenges. One such challenge is the detrimental effect of intermetallic sigma phase precipitation during hot working or annealing at temperatures between 650 °C and 950 °C. Sigma phase is a chromium- and molybdenum-rich intermetallic compound that is hard and brittle. Its formation depletes the surrounding ferrite grains of these crucial elements, leading to increased hardness, decreased ductility, reduced

impact toughness, and deterioration of corrosion resistance [1,8–16]. The harmful effect of sigma phase precipitation on mechanical properties is directly shown in this paper.

The SAF 2205 duplex stainless steel grade is the most widespread of the duplex grades. According to the literature, this steel is susceptible to degradation by sigma phase precipitation [1,14,15,17–19]. This study aims to analyze the degradation of mechanical properties in SAF 2205 during annealing in the temperature range from 600 to 750 °C. The temperature range was chosen to assess the damage that can be inflicted on DSS components during slow cooling or temporary overheating.

2. Materials and Methods

The chemical composition of the used SAF 2205 is given in Table 1. The samples were taken from 20 mm thick, 1 m wide plates; the as-received condition was solution-annealed. Isothermal annealing was performed in a resistance furnace (400 × 600 × 400 chamber) without a protective atmosphere at four different temperatures (600, 650, 700, and 750 °C) for four different annealing times (1 min, 10 min, 100 min, and 1000 min). A dummy sample (made from the same steel) with a thermocouple type K was added along with the studied material to monitor the temperature. The samples reached the studied temperature in around 10 min. The samples at first heated up quickly, but then approached the final temperature more slowly. Samples large enough to be made into tensile or impact toughness specimens are not heated up immediately after placing them in the furnace, so temperature must be carefully monitored. Additionally, at higher temperatures above 600 °C a lot of energy is transferred through radiation, so the thermocouple needs to be inserted in the sample; if the thermocouple is welded on the surface, the measured temperature will be much higher than the internal temperature of the sample.

Table 1. Chemical composition of SAF 2205 in wt. %.

C	Si	Mn	P	S	Cr	Ni	Cu	Mo	N
0.021	0.32	1.58	0.0026	0.002	22.95	5.3	0.26	2.74	0.14

The microstructure was characterized with an optical microscopy Nikon Microphot FXA microscope (Nikon, Minato City, Japan) with a 3CCD Hitachi HV-C20A camera (Hitachi, Ltd., Tokyo, Japan). Hardness (Vickers hardness HV10, Wilson Instruments, Norwood, MA, USA) was tested according to BS EN ISO 6507-1:2005 [20] using an Instron Tukon 2100B Vickers hardness measurement instrument (Wilson Instruments, Norwood, MA, USA). Five measurements were taken for each sample. The Charpy V-notch impact toughness was measured according to EN ISO 148-1:2017 [21] with a 300 J Charpy hammer; five specimens were tested for each heat treatment. Tensile tests were conducted according to EN ISO 6892-1:2017 [22] on an Instron 8802 universal testing machine (Wilson Instruments, Norwood, MA, USA); three round specimens (d_0 = 10 mm, L_0 = 50 mm) were tested for each heat treatment. The tensile tests were conducted at room temperature 23 ± 1 °C, with a test rate of 0.00025/s. The ferrite content measurement was taken using a Feritscope MP30 instrument according to EN ISO 17655:2003 [23]. The thermodynamic CALPHAD modeling was performed with Thermo-Calc version 2021b, TCFE10 Steels/Fe-alloys database (Thermo-Calc Software AB, Stockholm, Sweden).

3. Results and Discussion

The results showed the changing microstructure and mechanical properties according to the different annealing temperatures and times. The microstructural changes were the result of phase transformations that were driven by diffusion; therefore, time and temperature were the main driving factors for the changes. The authors would like to emphasize that this study dealt with heating up the samples and the results obtained with cooling them down may differ. The general trends are applicable for cooling phases in

industry; however, generally, overheating of DSS elements is less studied and can prove more dangerous in practice.

3.1. Thermocalc Calculations

The temperature range 500 to 1000 °C was used to present the stability of different phases in the SAF 2205 steel. The phase composition is presented in Figure 1a, with the more clearly presented details for carbide and nitride precipitation in Figure 1b. Due to the high percentage of ferrite, austenite, and sigma phases, the lines for the aforementioned phases are not visible, while the ferrite lines appear vertical. The stability of ferrite decreases from 55 wt. % at 500 °C to 0 wt. % at 666 °C, and starts to rise again at 860 °C to 46 wt. % at 940 °C, where it slowly rises to 49 wt. % at 1000 °C. The austenite, on the other hand, rises from the lowest point 10 wt. % at 500 °C to 63 wt. % at 666 °C, then slowly grows to the peak value of 77 wt. % at 857 °C. The percentage of austenite falls to 52.4 wt. % at 942 °C, and then slowly falls to 51 wt. % at 1000 °C. The most deleterious sigma phase is stable at 500 °C (32 wt. %), reaches the highest value at 35 wt. % and 666 °C, slowly falls down to 26 wt. % at 834 °C, and then more rapidly decreases to 0 wt. % at 941 °C. Although stable at lower temperatures, in practice the sigma phase usually precipitates above 700 °C [24]. While the chromium nitrides are stable in the whole temperature range, their value increases from 1 wt. % at 500 °C to the maximum of 1.2 wt. % at 651 °C, and then falls to 0.5 wt. % at 1000 °C. Chromium carbides $M_{23}C_6$, on the other hand, are stable up to 880 °C; their highest content in the studied temperature range is 0.4 wt. % at 500 °C. The nucleation of carbides is faster at lower temperatures, and the ferrite grain boundaries are the nucleation sites [17].
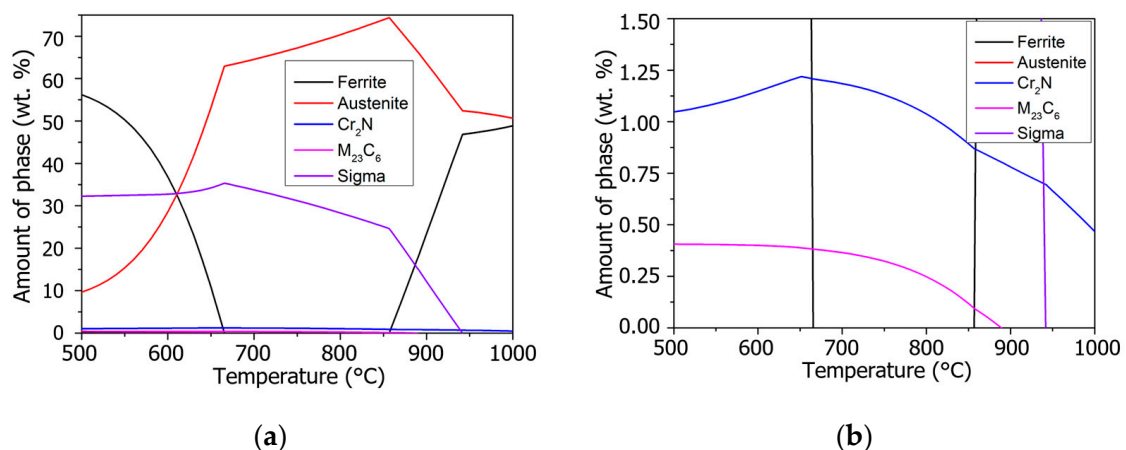

(**a**)   (**b**)

Figure 1. Equilibrium amount of thermodynamically stable phases in the temperature range from 500 to 1000 °C for SAF 2205. (**a**) Presentation of all the phases; (**b**) detailed presentation of carbide and nitride precipitation.

3.2. Vickers Hardness

Figure 2 presents the Vickers hardness measurements HV10 according to the different annealing temperatures and times. A slight increase in hardness was observed for all samples compared to the as-received condition (235 to 245 HV). No significant changes were detected at the lowest annealing temperatures (600 °C) for any duration, while there was a slight increase at 650 °C for 1000 min. A more pronounced increase in hardness due to sigma phase formation was observed after annealing at 750 °C for 1000 min (303 HV) with a further increase to 358 HV after 1000 min.
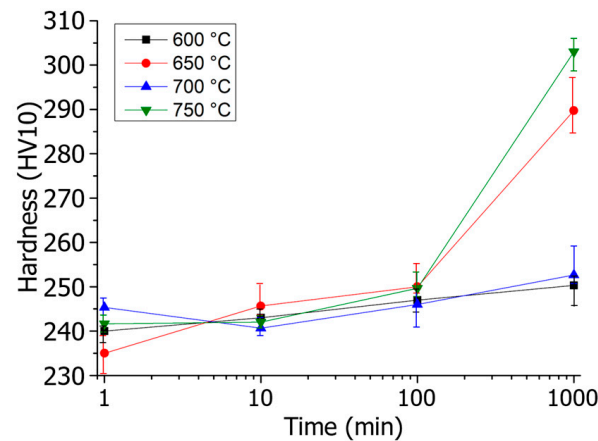
Figure 2. Vickers hardness HV10 for different annealing temperatures (600 to 750 °C) and times (1 to 1000 min).

3.3. Charpy V-Notch Impact Toughness

The Charpy V-notch impact toughness results (Figure 3) showed a more significant change in values than hardness. The as-received samples exhibited an impact toughness of approximately 300 J. The decrease in impact toughness after 1 and 10 min at 600, 650, and 700 °C was about the same, 250 J, while at 750 °C the decrease was over 90 J to 205 J. This means that just heating up to the working temperature in circa 10 min is enough to deteriorate the impact toughness. Longer annealing times (100 and 1000 min) at 600 and 650 °C decreased to 150 J and 60 J. At the highest temperature, the decrease was much worse and resulted in a toughness of only 43 J after 100 min, and the toughness was extremely low at 8 J after 1000 min. This significant reduction in impact toughness can be attributed to the embrittling effect of sigma phase formation at ferrite grain boundaries. The results show that even short times such as 1 min at 750 °C can be devastating for SAF 2205.
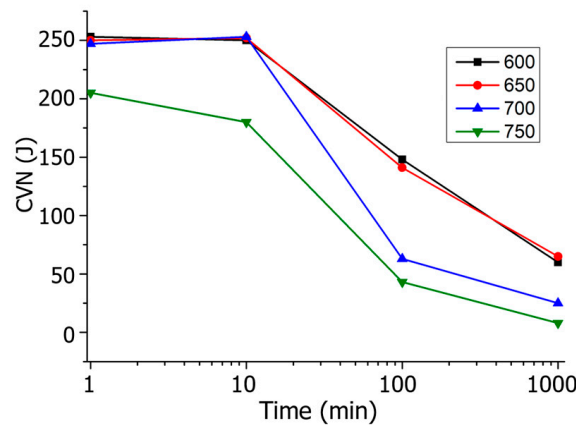

Figure 3. Charpy V-notch impact toughness for different annealing temperatures (600 to 750 °C) and times (1 to 1000 min).

3.4. Tensile Properties

The yield strength (Rp0.2) measurements (Figure 4) revealed no significant influence of annealing temperature and time within the investigated range. Deviations in yield strength ranged from 485 MPa to 521 MPa across all samples. Similarly, no increase in tensile strength (Figure 5) was observed after short annealing times (1 and 10 min). After longer durations (100 min), a moderate increase in Rm from 760 MPa to 785 MPa was observed, with a further increase to 850 MPa (16% increase) after 1000 min at 750 °C.
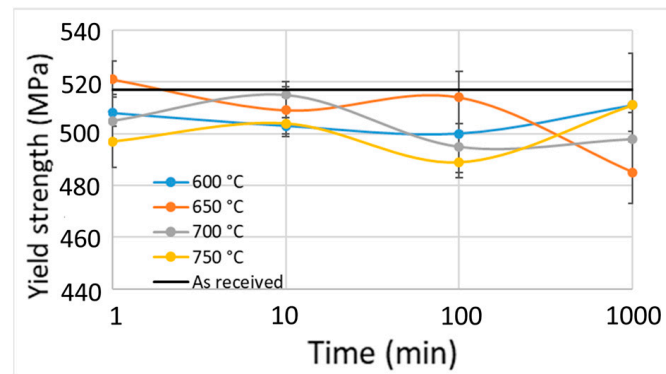
Figure 4. Influence of annealing time and temperature on the yield strength of SAF 2205.
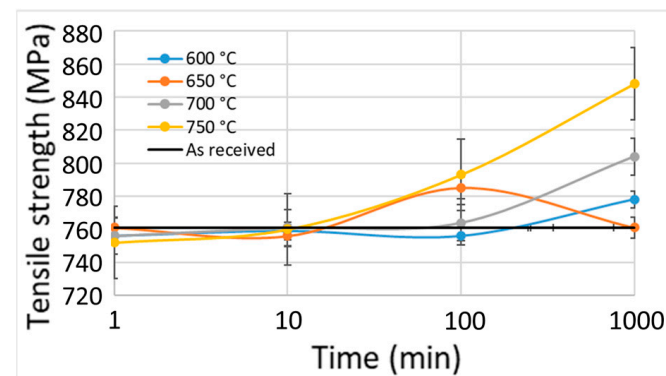

Figure 5. Influence of annealing time and temperature on the tensile strength of SAF 2205.

Elongation after fracture (Figure 6) showed no significant decrease for the shortest annealing times (1 and 10 min) compared to the as-received specimen (35% elongation). However, a decrease of 21% (27.7% elongation) was observed after 100 min of annealing at 750 °C. Elongation dropped to only 13.7% (61% decrease) at the longest annealing time. This decrease can be attributed to the reduced ductility caused by sigma phase formation.
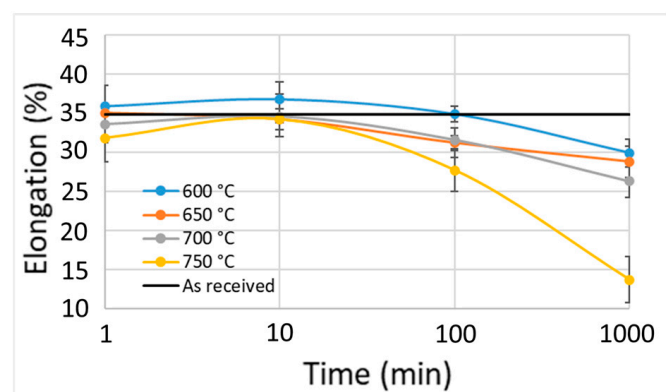

Figure 6. Influence of annealing time and temperature on the elongation of SAF 2205.

3.5. Microstructure and Sigma Phase Formation

Metallographic analysis was performed using Murakami's etchant at 60 °C for 20 s to reveal the microstructure. The grains were elongated in the rolling direction; they were approximately 20 μm wide and 100 μm long. Figure 7 shows the initial microstructure of the as-received sample, consisting of austenite (lighter phase) and ferrite (darker phase). Figure 8 presents the microstructure of the specimens annealed for 1000 min at all four temperatures. No sigma phase was observed after annealing at 600 °C. At 650 °C after

1000 min, some sigma phase precipitates were visible at ferrite grain boundaries. The amount of sigma phase and the depletion of ferrite increased with increasing annealing temperature. Figure 9 shows a higher magnification image of the microstructure after annealing at 750 °C for 1000 min, with austenite (A), delta ferrite (F), and sigma phase (σ) clearly marked.
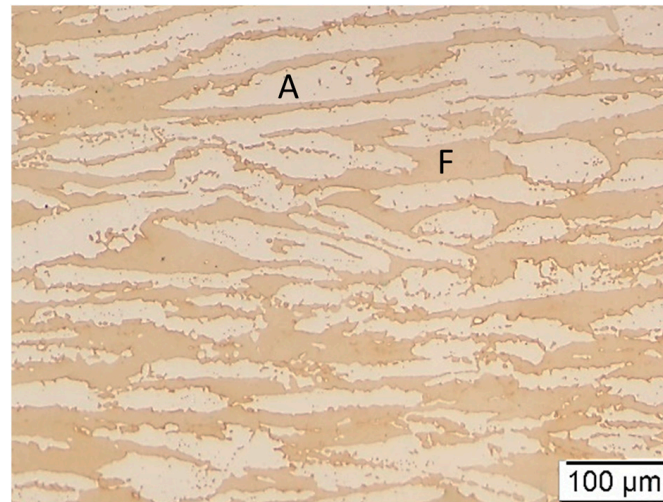

Figure 7. Initial microstructure of investigated steel in the as-received solution annealed condition, austenite (A) and ferrite (F).
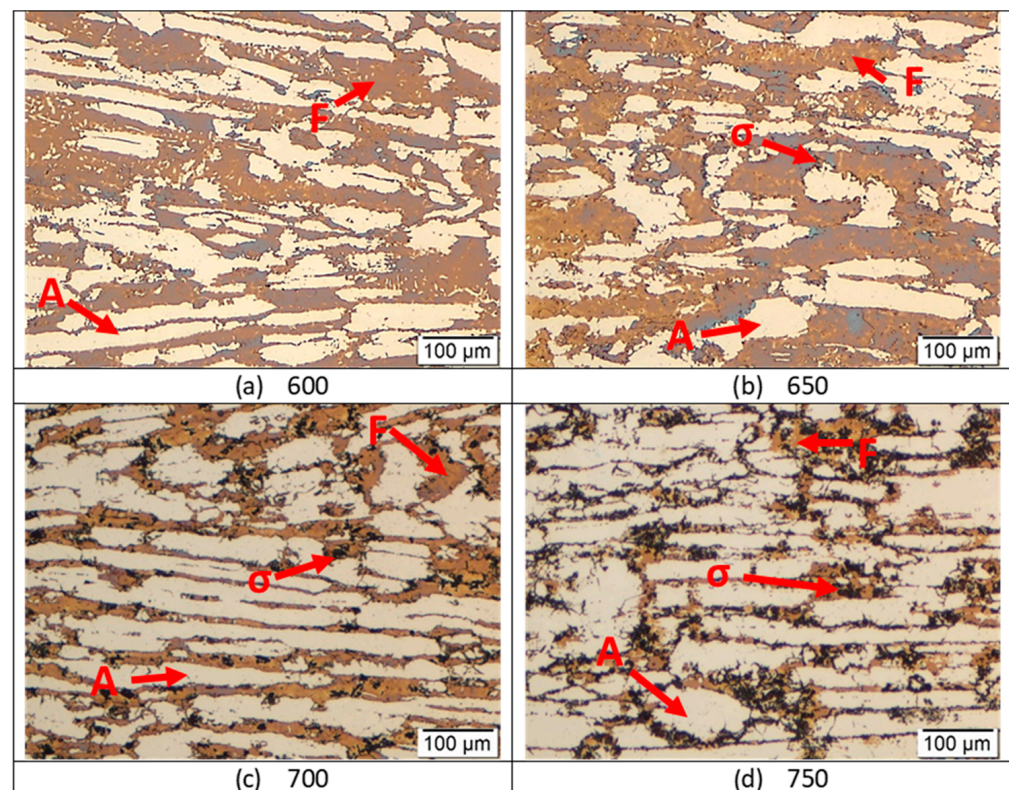

Figure 8. Microstructures of investigated SAF 2205 duplex stainless steel samples after annealing for 1000 min at four different temperatures with marked phases. A—austenite; F—ferrite; σ—sigma phase; (**a**) annealing at 600 °C; (**b**) annealing at 650 °C; (**c**) annealing at 700 °C; (**d**) annealing at 750 °C.
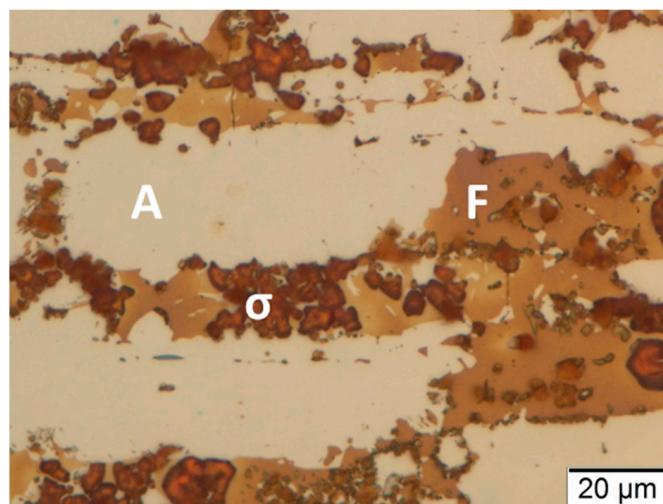
Figure 9. Microstructure of investigated SAF 2205 duplex stainless steel with a large amount of sigma phase after annealing for 1000 min at 750 °C with marked austenite (A), delta ferrite (F), and sigma phase (σ).

3.6. Ferrite Content

A feritscope was used to determine the ferrite-to-austenite ratio during annealing. The results are given in Table 2. The as-received specimen exhibited a balanced ratio of approximately 50:50. After 1 min of annealing at all temperatures, no significant changes were observed. After 10 min, the decrease in ferrite content became more evident at the highest annealing temperature (750 °C), dropping to 45%. After 100 min of annealing, the ferrite content remained around 50% at lower temperatures, while it dropped to 42% at 750 °C. The longest annealing time resulted in a further decrease in ferrite content to 45% at 600 °C and 650 °C and to 40% at 700 °C. However, at 750 °C for 1000 min, the ferrite content dropped significantly to only 16%. This substantial reduction in ferrite content can be attributed to the consumption of ferrite during sigma phase formation.

Table 2. Influence of annealing time and temperature on the ferrite content in SAF 2205 steel; ferrite contents given in wt. %.

t (min) \ T (°C)	600	650	700	750
1	50.1 ± 0.7	50.6 ± 0.5	51.1 ± 0.9	50.4 ± 0.6
10	51.1 ± 0.5	48.8 ± 0.5	46.9 ± 0.6	44.7 ± 0.8
100	52.3 ± 0.6	48.7 ± 0.7	45.9 ± 1.4	42.4 ± 1.2
1000	45.7 ± 1.5	47.2 ± 0.9	39.7 ± 2	15.9 ± 1.8

3.7. Fractography

The analyzed fracture surfaces of the Charpy specimens are shown in Figure 10. The lateral expansion of the specimens decreased with increasing temperature or prolonged annealing time. The appearance becomes almost entirely brittle after annealing at 750 °C for 1000 min (Figure 10). The microstructure near the fracture of the specimens after the longest annealing times at 600 °C and 650 °C (Figure 11) shows fragmented austenite, which is a consequence of deformation and material flow due to lateral expansion. At higher temperatures, transgranular crack propagation is evident, with no fragmentation of the austenite phase (Figure 11c,d). The SEM images reveal a relatively ductile fracture surface of the austenite with a serrated ferrite surface at lower temperatures of 600 and 650 °C, as shown for 650 °C and 1000 min in Figure 12a. The ferrite serration was not observed at 700 and 750 °C for 1000 min, as shown in Figure 12b (750 °C, 1000 min), but there was a distinct brittle fracture of the sigma phase. While ferrite is not serrated, both ferrite and austenite have smooth brittle appearances.
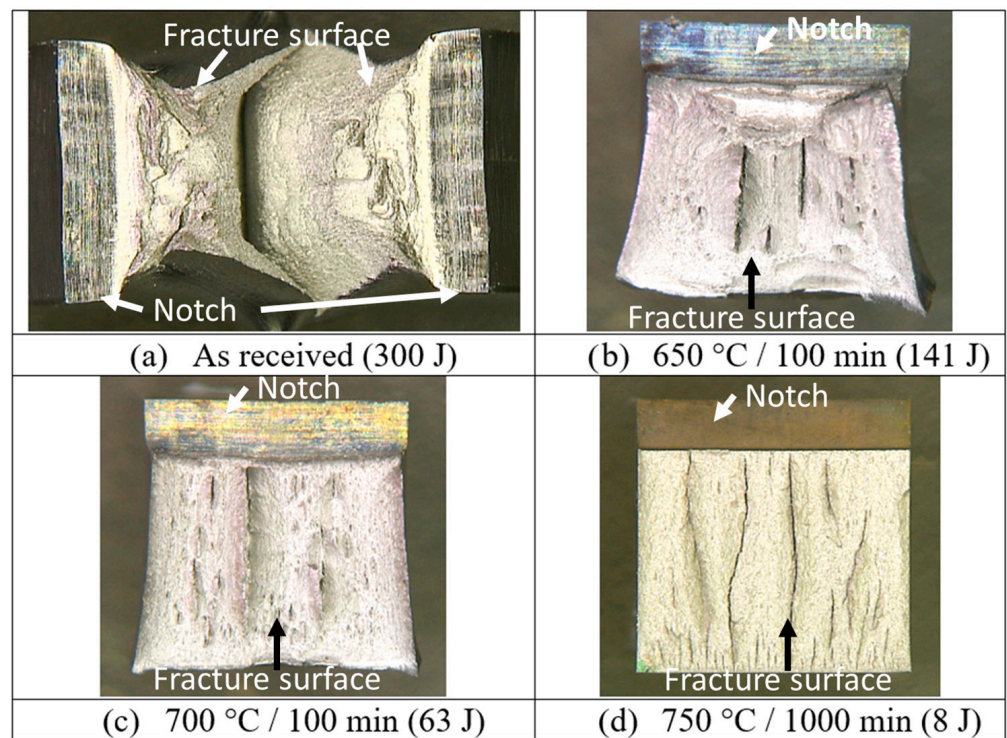
Figure 10. Fracture appearance of Charpy V-notch impact toughness specimens of SAF 2205 duplex stainless steel samples: (**a**) as-received condition—300 J; (**b**) annealed at 650 °C for 100 min—141 J; (**c**) annealed at 700 °C for 100 min—63 J; (**d**) annealed at 750 °C for 1000 min—8 J.
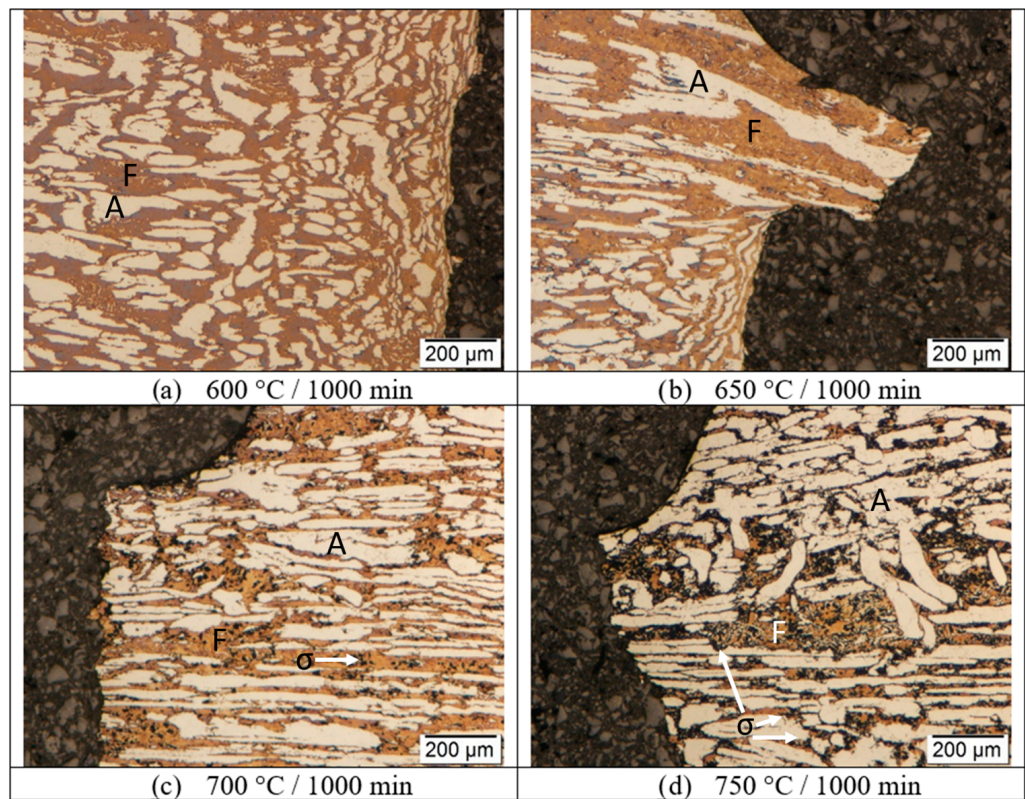

Figure 11. Crack propagation on Charpy V-notch impact toughness specimens after 1000 min of annealing at different temperatures: (**a**) 600 °C, (**b**) 650 °C, (**c**) 700 °C, (**d**) 750 °C, with marked austenite (A), delta ferrite (F), and sigma phase (σ).

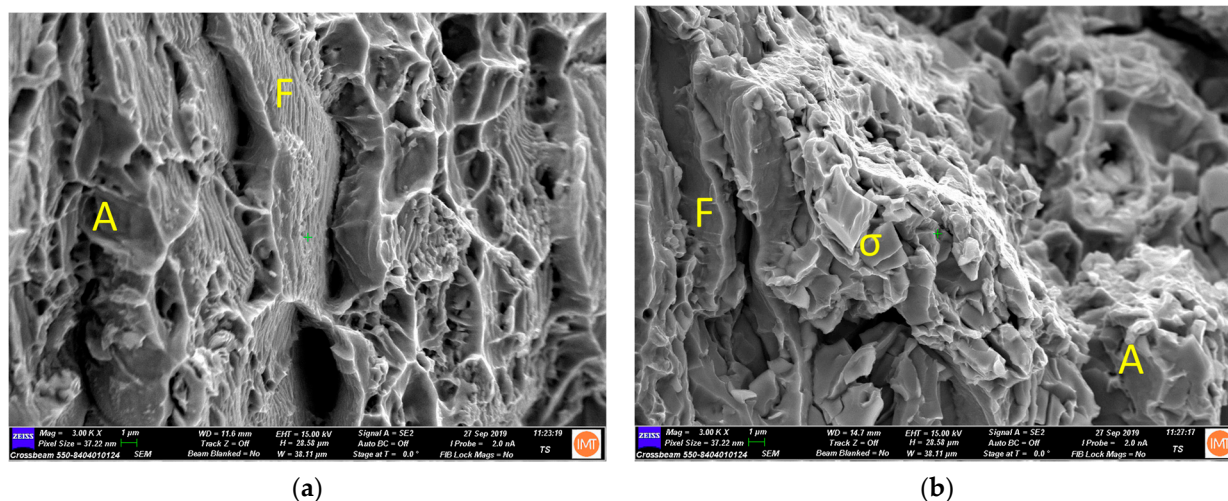**(a)**   **(b)**

Figure 12. Fracture surface of Charpy V-notch impact toughness specimens annealed at different conditions: (**a**) 650 °C for 1000 min, (**b**) 750 °C for 1000 min, with marked austenite (A), delta ferrite (F), and sigma phase (σ).

4. Conclusions

This study investigated the influence of isothermal annealing on the microstructure and mechanical properties of SAF 2205 duplex stainless steel. The findings show that the steel is not suitable for applications where higher temperatures are involved. In fact, even short-term overheating to 750 °C can be detrimental to its mechanical properties. The results highlight the detrimental effects of sigma phase precipitation on impact toughness and ductility, particularly at higher annealing temperatures and longer durations. These findings suggest that strict control of annealing parameters is crucial to preserve the desirable properties of SAF 2205 duplex stainless steel. This means the steel should be water-quenched after solution annealing. The following key conclusions can be drawn:

- The impact of annealing on impact toughness is significantly more pronounced compared to hardness. Even the initial heating and holding of the samples for 1 min resulted in a 25% lowering of the impact toughness. While hardness increased by a maximum of 25%, impact toughness decreased by more than 90%.
- Yield strength is not strongly affected by annealing, while tensile strength can increase up to 100 MPa and elongation can decrease by more than 50% in the case of annealing at 750 °C for 1000 min.
- Sigma phase formation is sluggish at lower temperatures (up to 650 °C). Only a few precipitates were observed after annealing at 650 °C for 1000 min. At higher temperatures, the precipitation rate increases, and ferrite decomposes faster. At 750 °C and 1000 min of annealing, the ferrite content dropped from approximately 50% to only 16%.

Author Contributions: Conceptualization, J.B.; methodology, B.Ž. and B.Š.B.; software, J.B.; investigation, J.B., B.Ž. and B.Š.B.; writing—original draft preparation, J.B. and B.Ž.; writing—review and editing, J.B.; visualization, J.B. and B.Ž. All authors have read and agreed to the published version of the manuscript.

Data Availability Statement: The data presented in this study are available in the article.

Conflicts of Interest: The authors declare no conflicts of interest.

References

1.   Wang, R. Precipitation of Sigma Phase in Duplex Stainless Steel and Recent Development on Its Detection by Electrochemical Potentiokinetic Reactivation: A Review. *Corros. Commun.* **2021**, *2*, 41–54. [CrossRef]

2.   Liu, J.; Han, J.; Lu, R. Study on descaling characteristics of 304 stainless steel using pickling and abrasive water jet. *Mater. Tehnol.* **2022**, *56*, 507–513. [CrossRef]

3.   Torkar, M.; Kocijan, A.; Celin, R.; Burja, J.; Podgornik, B. Metallographic Investigation and Corrosion Resistance of Welds of Ferritic Stainless Steels. *Mater. Tehnol.* **2016**, *50*, 829–834. [CrossRef]

4.   Garrison, W.M.; Amuda, M.O.H. Stainless Steels: Martensitic. *Ref. Modul. Mater. Sci. Mater. Eng.* **2017**, 8804–8810. [CrossRef]

5.   Niessen, F.; Apel, D.; Danoix, F.; Hald, J.; Somers, M.A.J. Evolution of Substructure in Low-Interstitial Martensitic Stainless Steel during Tempering. *Mater. Charact.* **2020**, *167*, 110494. [CrossRef]

6.   Patankar, S.N.; Lim, C.T.; Tan, M.J. Superplastic Forming of Duplex Stainless Steel. *Metall. Mater. Trans. A* **2000**, *31*, 2394–2396. [CrossRef]

7.   Tehovnik, F.; Žužek, B.; Burja, J. Hot Tensile Testing of SAF 2205 Duplex Stainless Steel. *Mater. Tehnol.* **2016**, *50*, 989–993. [CrossRef]

8.   Burja, J.; Tehovnik, F.; Vode, F.; Batic, B.Š. Phase Transformations during High Temperature Treatments in SAF 2205 Duplex Stainless Steel. In Proceedings of the ESSC and DUPLEX 2017—9th European Stainless Steel Conference—Science and Market and 5th European Duplex Stainless Steel Conference and Exhibition, Bergamo, Italy, 25–27 May 2017.

9.   Michalska, J.; Sozańska, M. Qualitative and Quantitative Analysis of σ and χ Phases in 2205 Duplex Stainless Steel. *Mater. Charact.* **2006**, *56*, 355–362. [CrossRef]

10. Huang, C.S.; Shih, C.C. Effects of Nitrogen and High Temperature Aging on Sigma Phase Precipitation of Duplex Stainless Steel. *Mater. Sci. Eng. A* **2005**, *402*, 66–75. [CrossRef]

11. Hosseini, V.A.; Karlsson, L.; Wessman, S.; Fuertes, N. Effect of Sigma Phase Morphology on the Degradation of Properties in a Super Duplex Stainless Steel. *Materials* **2018**, *11*, 933. [CrossRef] [PubMed]

12. Topolska, S.; Labanowski, J. Impact-Toughness Investigations of Duplex Stainless Steels. *Mater. Tehnol.* **2015**, *49*, 481–486. [CrossRef]

13. Tehovnik, F.; Burja, J.; Vode, F. Hot Tensile Tests and Phase Transformations in 2101 Lean Duplex Stainless Steel. In Proceedings of the ESSC and DUPLEX 2017—9th European Stainless Steel Conference—Science and Market and 5th European Duplex Stainless Steel Conference and Exhibition, Bergamo, Italy, 25–27 May 2017.

14. Nagar, R.; Patel, K.K.; Parmar, A. Study and Characterization of Sigma Phase in Duplex Stainless Steel 2205 (03Kh22N6M2). *Met. Sci. Heat Treat.* **2024**, *65*, 558–562. [CrossRef]

15. Biezma, M.V.; Martin, U.; Linhardt, P.; Ress, J.; Rodríguez, C.; Bastidas, D.M. Non-Destructive Techniques for the Detection of Sigma Phase in Duplex Stainless Steel: A Comprehensive Review. *Eng. Fail. Anal.* **2021**, *122*, 105227. [CrossRef]

16. Zhao, Y.; Zhou, E.; Xu, D.; Yang, Y.; Zhao, Y.; Zhang, T.; Gu, T.; Yang, K.; Wang, F. Laboratory Investigation of Microbiologically Influenced Corrosion of 2205 Duplex Stainless Steel by Marine Pseudomonas Aeruginosa Biofilm Using Electrochemical Noise. *Corros. Sci.* **2018**, *143*, 281–291. [CrossRef]

17. Redjaïmia, A.; Garcia, A.M.M. On the M23 C6-Carbide in 2205 Duplex Stainless Steel: An Unexpected (M23 C6/Austenite)—Eutectoid in the δ-Ferritic Matrix. *Metals* **2021**, *11*, 1340. [CrossRef]

18. Silva, E.M.; Marinho, L.B.; Rebouças Filho, P.P.; Leite, J.P.; Leite, J.P.; Fialho, W.M.L.; De Albuquerque, V.H.C.; Tavares, J.M.R.S. Classification of Induced Magnetic Field Signals for the Microstructural Characterization of Sigma Phase in Duplex Stainless Steels. *Metals* **2016**, *6*, 164. [CrossRef]

19. Gao, T.; Wang, J.; Sun, Q.; Han, P. Corrosion Behavior Difference in Initial Period for Hot-Rolled and Cold-Rolled 2205 Duplex Stainless Steels. *Metals* **2018**, *8*, 407. [CrossRef]

20. *BS EN ISO 6507-1:2005*; Metallic Materials—Rockwell Hardness Test—Part 1: Test Method. ISO: Geneva, Switzerland, 2015.

21. *EN ISO 148-1:2016*; Metallic Materials—Charpy Pendulum Impact Test—Part 1: Test Method. ISO: Geneva, Switzerland, 2016.

22. *EN ISO 6892-1:2017*; Metallic Materials—Tensile Testing—Part 1: Method of Test at Room Temperature. ISO: Geneva, Switzerland, 2017.

23. *EN ISO 17655:2003*; Method for Taking Samples for Delta Ferrite Measurement. ISO: Geneva, Switzerland, 2003.

24. Magnabosco, R. Kinetics of Sigma Phase Formation In a Duplex Stainless Steel. *Mater. Res.* **2009**, *12*, 321–327. [CrossRef]